Front. Phys. 10(6), 107405 (2015)
DOI 10.1007/s11467-015-0521-x

RESEARCH ARTICLE

Quasiparticle scattering interference in electron-doped cuprate superconductors

Shu-Hua Wang*, Shuang-Sheng Yang*, Huai-Song Zhao†, Feng Yuan‡

College of Physics, Qingdao University, Qingdao 266071, China

Corresponding authors. E-mail: †hszhao@qdu.edu.cn, ‡yuan@qdu.edu.cn

Received August 12, 2015; accepted October 10, 2015

By considering the nonmonotonic d-wave gap effect, the energy and momentum dependence of quasiparticle scattering interference is studied in the presence of a single impurity. It is shown that the pattern of the quasiparticle scattering peaks in the full Brillouin zone of electron-doped cuprate superconductors is very different from that in the hole-doped case described by the Octet model. This difference is the result of the nonmonotonic d-wave superconducting gap in the electron-doped case. As the energy increases, the position of the local peaks in the Brillouin zone moves rapidly. In particular, the characteristic peaks of the electron-doped cuprate superconductors appear between the antinodal and nodal directions, unlike in the hole-doped case.

Keywords cuprate superconductors

PACS numbers 74.62.Dh, 74.20.Mn, 74.25.Bt, 74.20.-z

Since its discovery, the electron-doped cuprate superconductor [1] has become a very important component in studying high-temperature superconductivity. There are many similarities between electron-doped and hole-doped cuprate superconductors, including the layered structure of the CuO_2 plane, the square lattice, and the strong doping dependence of physical properties. However, more significantly, differences in electron-doped and hole-doped cuprate superconductors have been found by a wide variety of measurement techniques [2, 3]. First, the electron-doped cuprate has lower superconducting transition temperature T_c than the hole-doped cuprate, with T_c less than 30 K in electron-doped cuprate superconductors compared with up to 130 K in the hole-doped cuprate case [4] (160 K under pressure [5]). Second, the parent compounds of cuprate superconductors are Mott insulators with an antiferromagnetic long-range order (AFLRO) [6]. The AFLRO of the hole-doped cuprate is destroyed quickly as the doping concentration increases, and disappears around a doping level of $\delta \approx 0.05$. Superconductivity then appears below T_c until the doping concentration $\delta \approx 0.27$. However, in the electron-doped case, the AFLRO exists over a wide range of electron doping concentrations, and even coexists with superconductivity over some range of the electron doping concentration [2, 7]. Third, a large body of experimental data show that the superconducting gap function of the hole-doped cuprate superconductors has a monotonic d-wave symmetry $\Delta_{\boldsymbol{k}} = \Delta(\cos k_x - \cos k_y)$ [8, 9], whereas the electron-doped case has a nonmonotonic d-wave superconducting gap function $\Delta_{\boldsymbol{k}} = \Delta[(\cos k_x - \cos k_y) + B(\cos 2k_x - \cos 2k_y)]$ [15–18]. The nonmonotonic d-wave gap leads to a significant reconstruction of the Fermi surface; the maximum gap is not at the antinodal point $[\pi, 0]$, but at the hot spot between the antinodal point $[\pi, 0]$ and nodal point $[\pi/2, \pi/2]$, whereas the maximum gap is at the antinodal point $[\pi, 0]$ in hole-doped cuprate superconductors. As a good supplement for understanding high-temperature superconductivity in hole-doped cuprate superconductors, it is very important to observe the physical properties of electron-doped cuprate superconductors, especially those which are different from the hole-doped case.

In unconventional superconductivity, the electron–electron interaction usually plays a crucial role in determining the physical properties, especially the electronic structure [10–14]. Therefore, we can obtain the key components of the electron–electron correlation by studying the electronic structure. The electronic structure in electron-doped cuprate superconductors shows apparent discrepancy from the hole-doped case because of the nonmonotonic d-wave gap function observed by angle-

*These authors contributed equally to this work.

resolved photoemission spectroscopy (ARPES) [15–17]. The intensity of the Fermi surface at the optimal doping concentration in the electron-doped cuprate superconductors is strongly depressed at the hot spot (the intersection of the Fermi surface with the antiferromagnetic Brillouin zone boundary) between antinodal point $[\pi, 0]$ and nodal point $[\pi/2, \pi/2]$. Moreover, the impurity is a useful way of probing the microscopic electronic structure in cuprate superconductors [19], and non-magnetic impurities can lead to strong pair-breaking effects with non-s-wave symmetry gaps. As a very powerful tool for studying the local impurity effect, scanning tunneling microscopy (STM) can probe the local atomic-scale quasiparticle properties around impurity positions in real-space by measuring the tip-sample differential tunneling conductance, which is proportional to the local density of states [20, 21]. In particular, a Fourier-transformed STM technique has been used to obtain momentum-space information of quasiparticles. Therefore, both real-space and momentum-space modulations of local density of states can be acquired simultaneously [22, 23]. The quasiparticle scattering interference phenomena characterized by the peaks in the local density of states is believed to be important (these include the physical processes dominating quasiparticle scattering, quasiparticle momentum-space structure, and dispersion). For the hole-doped cuprate superconductors, the quasiparticle scattering interference is well established [22], and the positions of the local scattering peaks move in the Brillouin zone with increasing energy, which can be described by the Octet model [23]. Theoretically, based on the phenomenological d-wave Bardeen–Cooper–Schrieffer (BCS) formalism [24–32], the properties of the quasiparticle and its related quasiparticle scattering interference phenomena have been studied by considering the effect of impurities. However, for electron-doped cuprate superconductors, neither a corresponding STM experiment nor a theory to study the quasiparticle scattering interference phenomena have been reported until now.

In our earlier work [33], we considered the monotonic d-wave symmetry gap and discussed the energy and momentum dependence of quasiparticle scattering interference for hole-doped cuprate superconductors in the presence of a single point-like impurity. This study was conducted within the framework of the renormalized Hubbard model, and some of the main features of STM experiments on hole-doped cuprate superconductors were well reproduced, including the energy dependence of the quasiparticle scattering interference pattern and dispersion along the nodal and antinodal directions. In this letter, we study the quasiparticle scattering interference of the electron-doped cuprate superconductors in the superconducting state with the nonmonotonic d-wave symmetry gap. We clearly show that the quasiparticle scattering interference pattern of the electron-doped cuprate superconductors is very different from that in the hole-doped case. Therefore, the Octet model cannot explain the unusual local quasiparticle peaks in electron-doped cuprate superconductors.

For cuprate superconductors, it is widely accepted that, although the superconducting pairing mechanism of the cuprate superconductors may be beyond the conventional electron–phonon mechanism, the form of the BCS with d-wave gap symmetry is valid in describing the superconducting state of the cuprate superconductors, as confirmed by the ARPES experiments [34]. Moreover, the characteristic feature of cuprate superconductors is the presence of the two-dimensional CuO_2 plane, and it seems evident that the unusual behavior occurs mainly in this square plane. Therefore, we use the BCS Hamiltonian

$$H = \sum_{\boldsymbol{k},\sigma}(\xi_{\boldsymbol{k}} - \mu)C^{\dagger}_{\boldsymbol{k}\sigma}C_{\boldsymbol{k}\sigma} - \sum_{\boldsymbol{k}}\Delta(\boldsymbol{k})(C_{\boldsymbol{k}\downarrow}C_{-\boldsymbol{k}\uparrow} + C^{\dagger}_{-\boldsymbol{k}\uparrow}C^{\dagger}_{\boldsymbol{k}\downarrow}), \tag{1}$$

where $\xi_{\boldsymbol{k}} = -2t_1(\cos\boldsymbol{k}_x + \cos\boldsymbol{k}_y) + 4t_2\cos\boldsymbol{k}_x\cos\boldsymbol{k}_y$, $t_1 = 0.38$ eV, $t_2 = 0.12$ eV [17, 35], $C^{\dagger}_{\boldsymbol{k}}(C_{\boldsymbol{k}})$ is the electron creation (annihilation) operator, μ is the chemical potential related to doping concentration, and $\Delta(\boldsymbol{k}) = \Delta[\gamma^{(d)}_{\boldsymbol{k}} + B\gamma^{(2d)}_{\boldsymbol{k}}]$ is the superconducting gap function with the nonmonotonic d-wave effect. Here, $\gamma^{(d)}_{\boldsymbol{k}} = (\cos\boldsymbol{k}_x - \cos\boldsymbol{k}_y)/2$, and the parameter B determines the strength of the next higher harmonics $\gamma^{(2d)}_{\boldsymbol{k}} = (\cos 2\boldsymbol{k}_x - \cos 2\boldsymbol{k}_y)/2$.

Following our previous work [33], we define the electron diagonal and off-diagonal Green's functions as

$$G(\boldsymbol{k}, \tau - \tau') = -\langle TC_{\boldsymbol{k}\sigma}(\tau)C^{\dagger}_{\boldsymbol{k}\sigma}(\tau')\rangle$$
$$\Gamma^{\dagger}(\boldsymbol{k}, \tau - \tau') = -\langle TC^{\dagger}_{-\boldsymbol{k}\uparrow}(\tau)C^{\dagger}_{\boldsymbol{k}\downarrow}(\tau')\rangle. \tag{2}$$

The electron diagonal and off-diagonal Green's functions can then be obtained in BCS form as [36]

$$G(\boldsymbol{k}, \omega) = \frac{U^2_{\boldsymbol{k}}}{\omega - E_{\boldsymbol{k}}} + \frac{V^2_{\boldsymbol{k}}}{\omega + E_{\boldsymbol{k}}}, \tag{3a}$$

$$\Gamma^{\dagger}(\boldsymbol{k}, \omega) = \frac{\Delta(\boldsymbol{k})}{2E_{\boldsymbol{k}}}\left(\frac{1}{\omega - E_{\boldsymbol{k}}} - \frac{1}{\omega + E_{\boldsymbol{k}}}\right), \tag{3b}$$

where $U^2_{\boldsymbol{k}} = [1 + (\xi_{\boldsymbol{k}} - \mu)/E_{\boldsymbol{k}}]/2$, $V^2_{\boldsymbol{k}} = [1 - (\xi_{\boldsymbol{k}} - \mu)/E_{\boldsymbol{k}}]/2$, and the quasiparticle spectrum $E_{\boldsymbol{k}} = \sqrt{(\xi_{\boldsymbol{k}} - \mu)^2 + \Delta^2(\boldsymbol{k})}$, $\Delta(\boldsymbol{k}) = \Delta[\gamma^{(d)}_{\boldsymbol{k}} + B\gamma^{(2d)}_{\boldsymbol{k}}]$.

To show the effect of the parameter B, we calculate the nonmonotonic d-wave superconducting gap function $\Delta(\boldsymbol{k})$ along the Fermi surface from the antinodal region

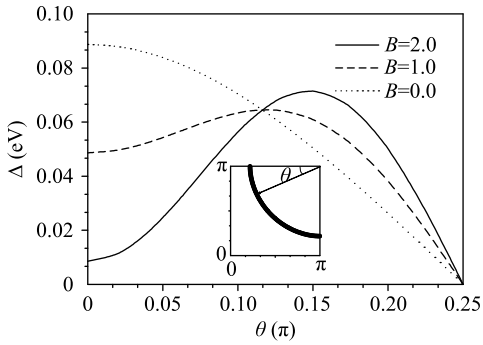

Fig. 1 The superconducting gap $\Delta(\boldsymbol{k}) = \Delta[\gamma_{\boldsymbol{k}}^{(d)} + B\gamma_{\boldsymbol{k}}^{(2d)}]|_{\boldsymbol{k}=\boldsymbol{k}_{\rm F}}$ along the Fermi surface as a function of the Fermi angle θ for $B = 0$ (*dotted line*), $B = 1.0$ (*dashed line*), $B = 2.0$ (*solid line*) with parameters $t_1 = 0.38$ eV, $t_2 = 0.12$ eV, $\Delta = 0.1$ eV, $\mu = 0.2$ eV. The dotted line ($B = 0$) is a monotonic d-wave gap. Inset: The corresponding Fermi angle in the Brillouin zone.

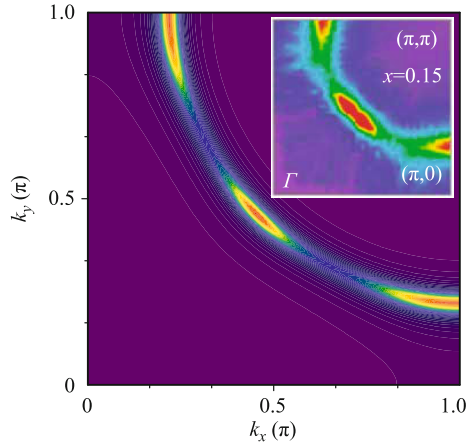

Fig. 2 The electron spectral function intensity maps at the Fermi energy ($\omega = 0$) in the Brillouin zone with parameters $t_1 = 0.38$ eV, $t_2 = 0.12$ eV, $\Delta = 0.1$ eV, $\mu = 0.2$ eV, $B = 2.0$. Inset: The corresponding ARPES experimental results of cuprate superconductors $Nd_{2-x}Ce_xCuO_{4+\delta}$, reproduced from Ref. [17].

$[\pi, 0]$ to the nodal region $[\pi/2, \pi/2]$ for different B, and plot $\Delta(\boldsymbol{k})$ as a function of the Fermi angle in Fig. 1.

Our results in Fig. 1 clearly show that there is a big change in the superconducting gap distribution along the Fermi surface for different B. When $B = 0$ (i.e., the monotonic d-wave gap form), the gap is largest near the antinodal point $[\pi, 0]$ at the Fermi momentum along the boundary of the Brillouin zone, and decreases monotonically with increasing Fermi angle, then vanishes near the nodal point $[\pi/2, \pi/2]$ at the Fermi momentum, which is the case for the hole-doped cuprate superconductors [9]. As B increases, the magnitude of the superconducting gap near $[\pi, 0]$ is suppressed, and the largest superconducting gap appears at the hot spot region (the intersection of the Fermi surface with the antiferromagnetic Brillouin zone boundary) between the antinodal point $[\pi, 0]$ and nodal point $[\pi/2, \pi/2]$. Therefore, the appearance of the parameter B also leads to the reconstruction of the Fermi surface.

The Fermi surface is a fundamental concept in condensed matter physics, and plays an important role in understanding the physical properties of a system. This is why we focus on the Fermi surface during the study of electron-doped cuprate superconductors. To study changes in the Fermi surface, we now discuss the electron spectrum of the electron-doped cuprate superconductors by calculating the electron spectral function $A(\boldsymbol{k}, \omega)$. The electron spectral function $A(\boldsymbol{k}, \omega)$ can be obtained from the electron diagonal Green's function $G(\boldsymbol{k}, \omega)$, $A(\boldsymbol{k}, \omega) = -2{\rm Im}G(\boldsymbol{k}, \omega)$. Therefore, from Eq. (3a), the electron spectral function $A(\boldsymbol{k}, \omega)$ is expressed as

$$A(\boldsymbol{k}, \omega) = [U_{\boldsymbol{k}}^2 \delta(\omega - E_{\boldsymbol{k}}) + V_{\boldsymbol{k}}^2 \delta(\omega + E_{\boldsymbol{k}})], \tag{4}$$

Information about the Fermi surface is then manifested by the electron spectral function at the Fermi energy, $A(\boldsymbol{k}, 0)$. In Fig. 2, we map the electron spectral function $A(\boldsymbol{k}, 0)$ at the Fermi energy with $t_1 = 0.38$ eV, $t_2 = 0.12$ eV, $\Delta = 0.1$ eV, $\mu = 0.2$ eV, and $B = 2.0$. For comparison, the corresponding ARPES experimental data for $Nd_{2-x}Ce_xCuO_{4+\delta}$ [17] is also shown in Fig. 2 (inset).

Our results clearly show that the Fermi surface of the electron-doped cuprate superconductors does not form a continuous contour in the Brillouin zone because of the suppression of the nonmonotonic d-wave superconducting gap. Obviously, the electron spectral distribution of the electron-doped cuprate superconductors at the Fermi momentum has the largest intensity near the antinodal point and nodal point, while it is suppressed at the hot spot (the intersection of the Fermi surface with the antiferromagnetic Brillouin zone boundary). This is in qualitative agreement with the experimental data [17]. The unusual behavior of the electron spectral distribution in the electron-doped cuprate superconductors is attributed to the effect of the nonmonotonic d-wave superconducting gap interacting with the next higher harmonic B, where the maximum of the superconducting gap is near the hot spot. In particular, the Fermi surface of the electron-doped cuprates is quite different from the hole-doped case, in which the electron spectral distribution reaches its maximum intensity at the nodal region and its minimum at the antinodal point [37].

Following our previous work [33], the full electron Green's function of the electron-doped cuprate superconductors can be expressed in Nambu representation as

$$\tilde{G}(\boldsymbol{k}, \omega) = \begin{pmatrix} G_(\boldsymbol{k}, \omega), & \Gamma(\boldsymbol{k}, \omega) \\ \Gamma^{\dagger}(\boldsymbol{k}, \omega), & -G(\boldsymbol{k}, -\omega) \end{pmatrix} \tag{5}$$

$$\tilde{G}(\boldsymbol{k},\omega)=\frac{\omega\tau_0+(\xi_{\boldsymbol{k}}-\mu)\tau_3+\Delta_{\boldsymbol{k}}\tau_1}{\omega^2-E_{\boldsymbol{k}}^2}, \tag{6}$$

where τ_0 is the unit matrix, τ_1 and τ_3 are Pauli matrices, and the tilde denotes a Nambu space matrix.

To investigate the effect of the quasiparticle scattering, we consider a single point-like impurity

$$\tilde{V}=V_0\delta(\boldsymbol{r})\tau_3, \tag{7}$$

which changes the full electron Green's function $\tilde{G}_{\rm I}(\boldsymbol{r},\boldsymbol{r}',\omega)$. With the impurity scattering contribution, this can be obtained from the T matrix [19] in real-space as

$$\tilde{G}_{\rm I}(\boldsymbol{r},\boldsymbol{r}',\omega)=\tilde{G}(\boldsymbol{r}-\boldsymbol{r}',\omega)+\tilde{G}(\boldsymbol{r},\omega)\tilde{T}(\omega)\tilde{G}(-\boldsymbol{r}',\omega) \tag{8}$$

where the T matrix can be obtained as [19]

$$\tilde{T}(\omega)=\frac{V_0\tau_3}{1-\tilde{G}(\omega)V_0\tau_3}. \tag{9}$$

In this case, the local density of states in real-space can be obtained as [33]

$$\tilde{N}(\boldsymbol{r},\omega)=-\frac{1}{\pi}{\rm Im}\tilde{G}_I(\boldsymbol{r},\omega)=\tilde{N}_0(\omega)+\delta\tilde{N}(\boldsymbol{r},\omega), \tag{10}$$

where $\tilde{N}_0(\omega)$ is the homogeneous density of states in the pure system, reflecting a homogeneous background, the second term $\delta\tilde{N}(\boldsymbol{r},\omega)$ is the modulation of the homogeneous density of states due to the appearance of the single point-like impurity, and $\delta N(\boldsymbol{r},\omega)=\delta\tilde{N}_{11}(\boldsymbol{r},\omega)$. Thus,

$$\delta N(\boldsymbol{r},\omega)=-\frac{1}{\pi}{\rm Im}[\tilde{G}(\boldsymbol{r},\omega)\tilde{T}(\omega)\tilde{G}(-\boldsymbol{r},\omega)]_{11}, \tag{11}$$

and the local density of states in momentum-space given by the Fourier transform is obtained as

$$\delta N(\boldsymbol{q},\omega)=-\frac{1}{\pi}{\rm Im}\left(\frac{1}{N}\sum_{\boldsymbol{k}}[\tilde{G}(\boldsymbol{k}+\boldsymbol{q},\omega)\tilde{T}(\omega)\tilde{G}(\boldsymbol{k},\omega)]_{11}\right). \tag{12}$$

We now discuss the quasiparticle scattering interference phenomena in electron-doped cuprate superconductors, and choose the parameters $t_1=0.38$ eV, $t_2=0.12$ eV, $\Delta=0.1$ eV, $\mu=0.2$ eV, and $B=2.0$. To determine the effect of the nonmonotonic d-wave superconducting gap on the quasiparticle scattering process, we calculate the momentum dependence of the Fourier-transformed local density of states $\delta N(\boldsymbol{q},\omega)$ for (a) the monotonic d-wave superconducting gap $\Delta(\boldsymbol{k})=\Delta\gamma_{\boldsymbol{k}}^{(d)}$ and (b) the nonmonotonic d-wave superconducting gap form $\Delta(\boldsymbol{k})=\Delta[\gamma_{\boldsymbol{k}}^{(d)}+B\gamma_{\boldsymbol{k}}^{(2d)}]$ with energy $\omega=-0.04$ eV in the presence of a single point-like potential scatterer of strength $V=0.5$ eV. The results are plotted in Fig. 3.

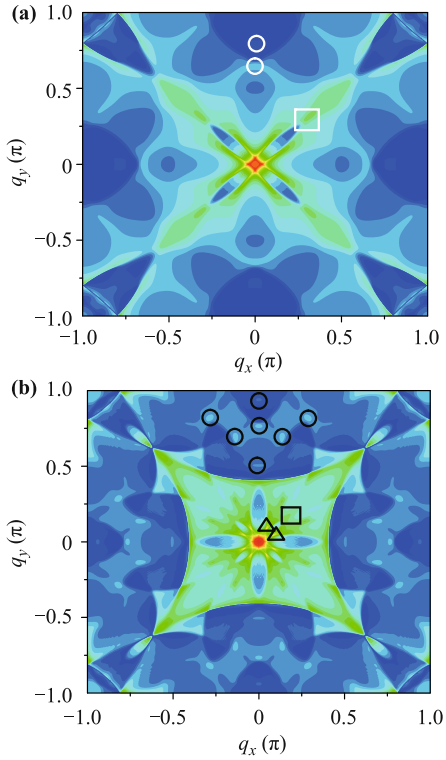

Fig. 3 The Fourier-transformed local density of states as a function of momentum in the full Brillouin zone with energy $\omega=-0.04$ eV for **(a)** the monotonic d-wave gap $\Delta(\mathbf{k})=\Delta\gamma_{\boldsymbol{k}}^{(d)}$ and **(b)** the nonmonotonic d-wave gap form $\Delta(\boldsymbol{k})=\Delta[\gamma_{\boldsymbol{k}}^{(d)}+B\gamma_{\boldsymbol{k}}^{(2d)}]$ in the presence of a single point-like potential scatterer of strength $V=0.5$ eV.

It is clear that there is a large difference between the patterns of quasiparticle scattering for the monotonic d-wave gap and the nonmonotonic d-wave gap. The results of $|\delta N(\boldsymbol{q},\omega)|$ are fourfold symmetric, and some local peaks (bright region) appear at different wavevectors $\boldsymbol{q}$. In particular, the local peaks, which are located in the antinodal direction ($[0,0]\rightarrow[\pi,0]$) with large momentum wavevectors $\boldsymbol{q}$ and the nodal direction ($[0,0]\rightarrow[\pi,\pi]$) with small momentum wavevectors $\boldsymbol{q}$, are often investigated because they reflect key information about the Fermi surface. In Fig. 3(a), there are four local peaks, marked by the white circles, at the antinodal region of one quarter Brillouin zone. The characteristic peak is marked by the white square along the nodal direction of one quarter Brillouin zone with the small wavevectors $\boldsymbol{q}$. With the monotonic d-wave gap, all these local peaks can be explained well by the Octet model [22, 33]. We now discuss the case of the nonmonotonic d-wave gap in electron-doped cuprate superconductors, shown in Fig. 3(b). There are approximately seven distinct local peaks at the antinodal region of one quar-

ter Brillouin zone, marked as black circles. In the nodal region with small momentum wavevectors $\boldsymbol{q}$, we can see a local peak, as in the monotonic d-wave case. In particular, two local peaks appear along the direction between the nodal direction and antinodal direction, where no peak was found under the monotonic d-wave gap. These are marked by the black triangles.

The pattern of the Fourier-transformed local density of states $|\delta N(\boldsymbol{q},\omega)|$, which embodies the quasiparticle scattering process, is strongly energy dependent. Thus, the position and magnitude of the local peaks in the pattern changes rapidly as the energy ($|\omega|$) increases. To illustrate these points clearly, the Fourier-transformed local density of states $|\delta N(\boldsymbol{q},\omega)|$ were evaluated as functions of energy and momentum. The results at various energies in the presence of a single point-like impurity potential scatterer of strength $V = 0.5$ J are plotted in Fig. 4. Our results show that the pattern of $|\delta N(\boldsymbol{q},\omega)|$ changes as the energy ($|\omega|$) increases. The positions of the local peaks in momentum-space vary, especially in the large-momentum antinodal region and the small-momentum nodal region. Analogous to Fig. 3, we mark the characteristic local peaks with the nonmonotonic d-wave superconducting gap using white circles, black circles, black squares, and black triangles. As the energy increases, the peaks in the antinodal region, marked by white circles, move toward the region of large momentum, away from the center of the Brillouin zone. In contrast, the peaks marked as black circles move toward the axis $[0,0] \rightarrow [\pi,0]$, and merge with the middle peak on the axis $[0,0] \rightarrow [\pi,0]$ at high energy. In the nodal direction, the peak marked by the black square moves toward large q along $[0,0] \rightarrow [\pi,\pi]$. The four characteristic peaks q_2, q_3, q_4, q_{14} marked with different colored arrows correspond to the arrows in Fig. 5(b). In particular, there is a peak marked by a black triangle in Fig. 4(b) between the antinodal direction $[0,0] \rightarrow [\pi,0]$ and nodal direction $[0,0] \rightarrow [\pi,\pi]$. This moves steadily toward large q as the energy increases.

Unlike the hole-doped cuprate superconductors with a monotonic d-wave superconducting gap $\Delta(\boldsymbol{k}) = \Delta\gamma_{\boldsymbol{k}}^{(d)}$, the superconducting gap of the electron-doped cuprate superconductors exhibits a nonmonotonic d-wave form $\Delta(\boldsymbol{k}) = \Delta[\gamma_{\boldsymbol{k}}^{(d)} + B\gamma_{\boldsymbol{k}}^{(2d)}]$. This leads to a significant difference in quasiparticle scattering interference between the hole-doped and electron-doped cuprate superconductors in the presence of a single point-like impurity. Both the hole-doped and electron-doped cuprate superconductors have nodes in the Brillouin zone where the superconducting gap is zero. Therefore, the impurity can induce a finite density of quasiparticle excitations in the gapless nodes, even at zero temperature [38]. These quasiparti-

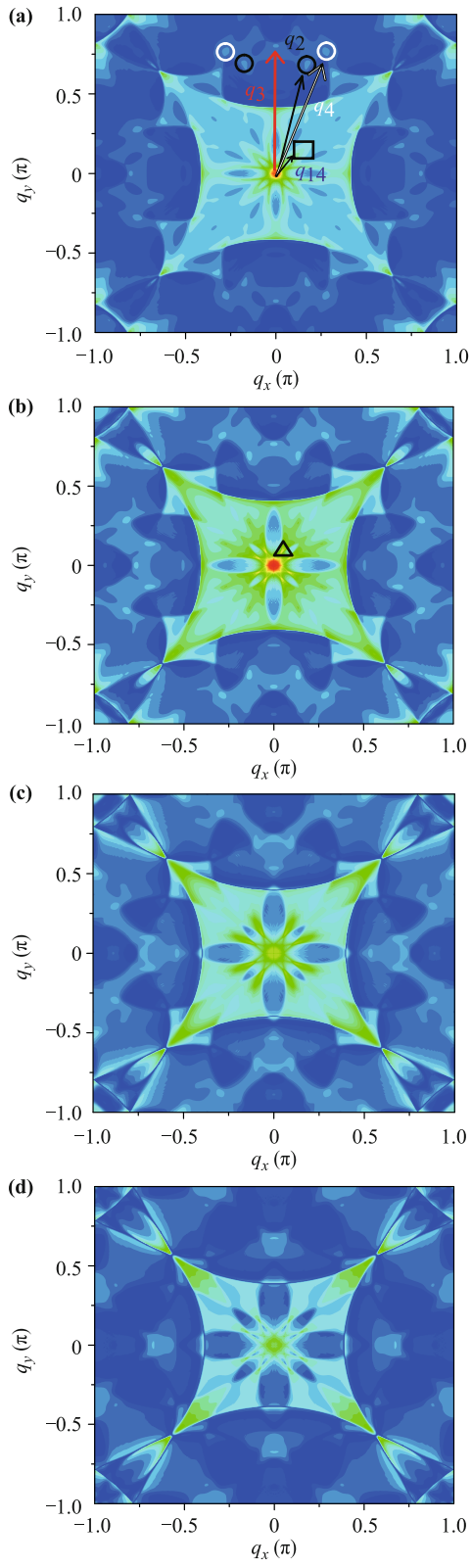

Fig. 4 The Fourier-transformed local density of states as a function of momentum in the full Brillouin zone with energy **(a)** $\omega = -0.03$ eV, **(b)** $\omega = -0.04$ eV, **(c)** $\omega = -0.05$ eV, and **(d)** $\omega = -0.06$ eV with parameters $t_1 = 0.38$ eV, $t_2 = 0.12$ eV, $\Delta = 0.1$ eV, $\mu = 0.2$ eV, $B = 2.0$ in the presence of a single point-like potential scatterer of strength $V = 0.5$ J.

cles induced by the impurity can also be scattered by the impurity. The quasiparticle dispersion in the superconducting state has been obtained as $E_{\boldsymbol{k}} = \sqrt{(\xi_{\boldsymbol{k}} - \mu)^2 + \Delta_{\boldsymbol{k}}^2}$. This gives $\Delta_{\boldsymbol{k}} = \Delta\gamma_{\boldsymbol{k}}^{(d)}$ in the hole-doped cuprate superconductors, and $\Delta(\boldsymbol{k}) = \Delta[\gamma_{\boldsymbol{k}}^{(d)} + B\gamma_{\boldsymbol{k}}^{(2d)}]$ in the electron-doped cuprate superconductors. The contours of constant energy (CCE) can be used to understand the electron structure of the system. Therefore, we calculated the CCE in the momentum space for (a) hole-doped ($B = 0$) and (b) electron-doped ($B = 2.0$) cuprate superconductors, and have plotted the results as a function of momentum in Fig. 5 for $t_1 = 0.38$ eV, $t_2 = 0.12$ eV, $\Delta = 0.1$ eV, and $\mu = 0.2$ eV. For the hole-doped cuprate superconductors, the quasiparticle dispersion $E_{\boldsymbol{k}}$ has a "banana-shaped" CCE surrounding the d-wave nodes [Fig. 5(a)], and the pattern of $|\delta N(\boldsymbol{q}, \omega)|$ representing the quasiparticle scattering process can be described well by the Octet model [23, 33], which has seven characteristic wavevectors (q_1, q_2, q_3, q_4, q_5, q_6, q_7). As the energy increases, the size of the CCE increases, which changes the magnitude of the characteristic wavevector and leads to movement in the local peaks. However, for electron-doped cuprate superconductors, the pattern of $|\delta N(\boldsymbol{q}, \omega)|$ is more complex than the hole-doped case, and cannot be understood within the Octet model. From Fig. 5(b), we can see that the CCE has a minimum in the hot spot region as a result of the higher harmonics $\gamma_{\boldsymbol{k}}^{(2d)} = (\cos 2k_x - \cos 2k_y)/2$, and the number of characteristic wavevectors at energy ω has fifteen wavevectors (q_1, q_2, q_3, q_4, q_5, q_6, q_7, q_8, q_9, q_{10}, q_{11}, q_{12}, q_{13}, q_{14}, q_{15}). As the energy increases, the size of the CCE increases in both the nodal and antinodal regions, and the related local peaks change position in the Brillouin zone.

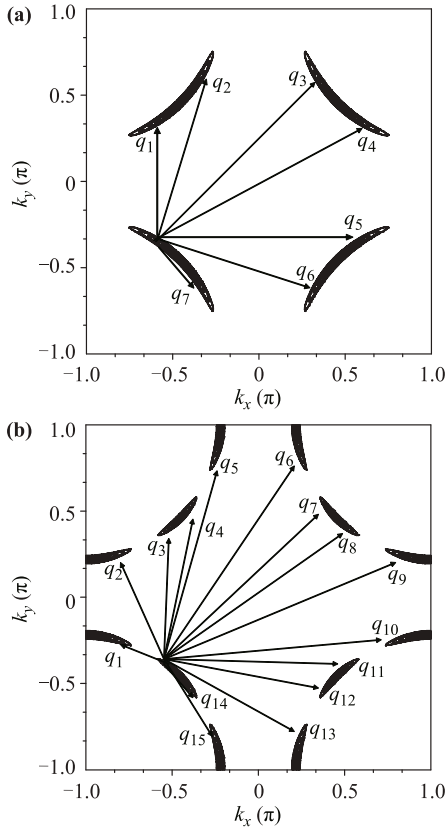

Fig. 5 Schematic plot of the contours of constant energy (CCE) in the first Brillouin zone for **(a)** hole-doped ($B = 0$) and **(b)** electron-doped ($B = 2.0$) cuprate superconductors. The characteristic wavevectors in the figures indicate elastic quasiparticle scattering processes.

To summarize, we first discussed the reconstruction of the Fermi surface in the electron-doped cuprate superconductors as a result of the nonmonotonic d-wave gap effect. The intensity of the electron spectral distribution was found to be strongly suppressed in the hot spot region. Second, the quasiparticle scattering interference phenomena of the electron-doped cuprate superconductors was discussed in the presence of a single impurity by calculating the energy and momentum dependence of the Fourier-transformed local density of states in the full Brillouin zone. It was shown that the nonmonotonic d-wave gap plays a crucial role in determining the pattern of the Fourier-transformed local density of states, which is very different from the pattern in the hole-doped case. In particular, there are several characteristic local peaks along the direction between the antinodal direction and nodal direction in electron-doped cuprate superconductors, and these local peaks do not appear in the hole-doped case. Moreover, as the energy increased, the position of the local peaks at both the antinodal and nodal regions in the Brillouin zone changed visibly. Our theoretical results predict the main features of quasiparticle scattering interference in the electron-doped cuprates, which is an important part of understanding the unusual physical properties of cuprate superconductors.

Acknowledgements This work was supported by the funds from the National Natural Science Foundation of China under Grant Nos. 10774082 and 11447144.

References

1. Y. Tokura, H. Takagi, and S. Uchida, A superconducting copper oxide compound with electrons as the charge carriers, *Nature* 337, 345 (1989)
2. N. P. Armitage, P. Fourier, and R. L. Greene, Progress and perspectives on electron-doped cuprates, *Rev. Mod. Phys.* 82(3), 2421 (2010)
3. A. Damascelli, Z. Hussain, and Z.-X. Shen, Angle-resolved photoemission studies of the cuprate superconductors, *Rev.*

Mod. Phys. 75(2), 473 (2003)

4. A. Schilling, M. Cantoni, J. D. Guo, and H. R. Ott, Superconductivity above 130 K in the Hg−Ba−Ca−Cu−O system *Nature* 363(6424), 56 (1993)
5. C. W. Chu, L. Gao, F. Chen, Z. J. Huang, R. L. Meng, and Y. Y. Xue, Superconductivity above 150 K in $HgBa_2Ca_2Cu_3O_{8+\delta}$ at high pressures, *Nature* 365(6444), 323 (1993)
6. M. A. Kastner, R. J. Birgeneau, G. Shirane, and Y. Endoh, Magnetic, transport, and optical properties of monolayer copper oxides, *Rev. Mod. Phys.* 70(3), 897 (1998)
7. Y. Krockenberger, J. Kurian, A. Winkler, A. Tsukada, M. Naito, and L. Alff, Superconductivity phase diagrams for the electron-doped cuprates $R_{2-x}Ce_xCuO_4$(R = La, Pr, Nd, Sm, Eu), *Phys. Rev. B* 77(6), R060505 (2008)
8. C. C. Tsuei and J. R. Kirtley, Pairing symmetry in cuprate superconductors, *Rev. Mod. Phys.* 72(4), 969 (2000)
9. H. Ding, M. R. Norman, J. C. Campuzano, M. Randeria, A. F. Bellman, T. Yokoya, T. Takahashi, T. Mochiku, and K. Kadowaki, Angle-resolved photoemission spectroscopy study of the superconducting gap anisotropy in $Bi_2Sr_2CaCu_2O_{8+x}$, *Phys. Rev. B* 54(14), R9678 (1996)
10. M. Guidry and Y. Sun, Superconductivity and superfluidity as universal emergent phenomena, *Front. Phys.* 10(4), 107404 (2015)
11. X.-G. Xu and W. Li, Electronic and magnetic structures of ternary iron telluride KFe_2Te_2, *Front. Phys.* 10(4), 107403 (2015)
12. W. Li, C. Setty, X. H. Chen, and J. P. Hu, Electronic and magnetic structures of chain structured iron selenide compounds, *Front. Phys.* 9(4), 471 (2014)
13. Y. Liang, X. X. Wu, W.-F. Tsai, and J. P. Hu, Pairing symmetry in layered BiS_2 compounds driven by electron-electron correlation, *Front. Phys.* 9(2), 199 (2014)
14. Y. Xing, Y. Sun, M. Singh, Y.-F. Zhao, M. H. W. Chan, and J. Wang, Electronic transport properties of topological insulator films and low dimensional superconductors, *Front. Phys.* 8(5), 508 (2013)
15. H. Matsui, K. Terashima, T. Sato, T. Takahashi, M. Fujita, and K. Yamada, Direct observation of a nonmonotonic $d_{x^2-y^2}$ wave superconducting gap in the electron-doped high-T_c superconductor $Pr_{0.89}LaCe_{0.11}CuO_4$, *Phys. Rev. Lett.* 95(1), 017003 (2005)
16. N. P. Armitage, D. H. Lu, C. Kim, A. Damascelli, K. M. Shen, F. Ronning, D. L. Feng, P. Bogdanov, Z.-X. Shen, Y. Onose, Y. Taguchi, Y. Tokura, P. K. Mang, N. Kaneko, and M. Greven, Anomalous electronic structure and pseudogap effects in $Nd_{1.85}Ce_{0.15}CuO_4$, *Phys. Rev. Lett.* 87(14), 147003 (2001)
17. N. P. Armitage, F. Ronning, D. H. Lu, C. Kim, A. Damascelli, K. M. Shen, D. L. Feng, H. Eisaki, and Z. X. Shen, Doping dependence of an n-type cuprate superconductor investigated by angle-resolved photoemission spectroscopy, *Phys. Rev. Lett.* 88(25), 257001 (2002)
18. E. H. da Silva Netoz, R. Cominz, Feizhou He, R. Sutarto, Yeping Jiang, R. L. Greene, G. A. Sawatzky, and A. Damascelli, Charge ordering in the electron-doped superconductor $Nd_{2-x}Ce_xCuO_4$, *Science* 347(6219), 282 (2015)
19. A. V. Balatsky, I. Vekhter, and J. X. Zhu, Impurity-induced states in conventional and unconventional superconductors, *Rev. Mod. Phys.* 78(2), 373 (2006)
20. Ø. Fischer, M. Kugler, I. Maggio-Aprile, C. Berthod, and C. Renner, Scanning tunneling spectroscopy of high-temperature superconductors, *Rev. Mod. Phys.* 79(1), 353 (2007)
21. I. M. Vishik, E. A. Nowadnick, W. S. Lee, Z. X. Shen, B. Moritz, T. P. Devereaux, K. Tanaka, T. Sasagawa, and T. Fujii, A momentum-dependent perspective on quasiparticle interference in $Bi_2Sr_2CaCu_2O_{8+\delta}$, *Nat. Phys.* 5(10), 718 (2009)
22. J. E. Hoffman, K. McElroy, D.-H. Lee, K. M. Lang, H. Eisaki, S. Uchida, and J. C. Davis, Imaging quasiparticle interference in $Bi_2Sr_2CaCu_2O_{8+\delta}$, *Science* 297(5584), 1148 (2002)
23. K. McElroy, R. W. Simmonds, J. E. Hoffman, D.-H. Lee, J. Orenstein, H. Eisaki, S. Uchida, and J. C. Davis, Relating atomic-scale electronic phenomena to wave-like quasiparticle states in superconducting $Bi_2Sr_2CaCu_2O_{8+\delta}$, *Nature* 422(6932), 592 (2003)
24. Q.-H. Wang and D.-H. Lee, Quasiparticle scattering interference in high-temperature superconductors, *Phys. Rev. B* 67(2), 020511 (2003)
25. J.-X. Zhu, A. V. Balatsky, T. P. Devereaux, Qimiao Si, J. Lee, K. McElroy, and J. C. Davis, Fourier-transformed local density of states and tunneling into a d-wave superconductor with bosonic modes, *Phys. Rev. B* 73(1), 014511 (2006)
26. D. Zhang and C. S. Ting, Energy-dependent modulations in the local density of states of the cuprate superconductors, *Phys. Rev. B* 67(10), 100506 (2003)
27. T. S. Nunner, W. Chen, B. M. Andersen, A. Melikyan, and P. J. Hirschfeld, Fourier transform spectroscopy of d-wave quasiparticles in the presence of atomic scale pairing disorder, *Phys. Rev. B* 73(10), 104511 (2006)
28. B. Liu, X. Yan, and F. Yuan, Electron correlation and impurity-induced quasiparticle resonance states in cuprate superconductors, *Journal of the Physical Society of Japan* 82(10), 114713 (2013)
29. B. Liu, X. Yan, and F. Yuan, Quasiparticle resonance states induced by a nonmagnetic impurity in Gossamer superconductors, *Solid State Communications* 177, 123 (2014)
30. B. Liu and Y. Liang, Density of states and nonmagnetic impurity effects in electron-doped cuprates, *Phys. Rev. B* 77(24), 245121 (2008)
31. B. Liu, Spin-resolved impurity resonance states in electron-doped cuprate superconductors, *Phys. Rev. B* 79(17), 172501 (2009)
32. Z. P. Huang, X. X. Wan, and F. Yuan, Local density of states

around two nonmagnetic impurities in cuprate superconductors, *Front. Phys.* 6(3), 309 (2011)

33. S. H. Wang, H. S. Zhao, and F. Yuan, Quasiparticle scattering interference in the renormalized Hubbard model, *Front. Phys.* 10(1), 107401 (2015)
34. H. Matsui, T. Sato, T. Takahashi, S. C. Wang, H. B. Yang, H. Ding, T. Fujii, T. Watanabe, and A. Matsuda, BCS-Like Bogoliubov quasiparticles in high-T_c superconductors observed by angle-resolved photoemisson spectroscopy, *Phys. Rev. Lett.* 90(21), 217002 (2003)
35. A. Hackl and S. Sachdev, Nernst effect in the electron-doped cuprate superconductors, *Phys. Rev. B* 79(23), 235124 (2009)
36. J. Bardeen, L. N. Cooper, and J. R. Schrieffer, Theory of superconductivity, *Phys. Rev.* 108(5), 1175 (1957)
37. Jian-Qiao Meng, M. Brunner, K.-H. Kim, H.-G. Lee, S.-I. Lee, J. S. Wen, Z. J. Xu, G. D. Gu, and G.-H. Gweon, Momentum-space electronic structures and charge orders of the high-temperature superconductors $Ca_{2-x}Na_xCuO_2Cl_2$ and $Bi_2Sr_2CaCu_2O_{8+\delta}$, *Phys. Rev. B* 84(6), 060513(R) (2011)
38. A. C. Durst and P. A. Lee, Impurity-induced quasiparticle transport and universal-limit Wiedemann–Franz violation in d-wave superconductors, *Phys. Rev. B* 62(2), 1270 (2000)